論文 / 著書情報
Article / Book Information

題目(和文)	ゴムフィルムへの微粒子付着におけるメニスカス形成および微粒子沈降
Title(English)	Microsphere Adhesion on Rubber Films Accompanied by Meniscus Formation and Sedimentation
著者(和文)	三島翔子
Author(English)	Shoko Mishima
出典(和文)	学位:博士(工学), 学位授与機関:東京工業大学, 報告番号:甲第11451号, 授与年月日:2020年3月26日, 学位の種別:課程博士, 審査員:扇澤 敏明,鞠谷 雄士,安藤 慎治,淺井 茂雄,松本 英俊
Citation(English)	Degree:Doctor (Engineering), Conferring organization: Tokyo Institute of Technology, Report number:甲第11451号, Conferred date:2020/3/26, Degree Type:Course doctor, Examiner:,,,,
学位種別(和文)	博士論文
Category(English)	Doctoral Thesis
種別(和文)	要約
Type(English)	Outline

Microsphere Adhesion on Rubber Films Accompanied by Meniscus Formation and Sedimentation

(ゴムフィルムへの微粒子付着におけるメニスカス形成および微粒子沈降)

Shoko Mishima

School of Materials and Chemical Technology, Department of Materials Science and Engineering

Tokyo Institute of Technology

1. Introduction

Pressure-sensitive adhesive (PSA) is a common means of adhesion used in various fields. Examples of daily use include adhesive tape or sticky paper. PSAs are also used in industrial fields such as building materials and cars. However, the phenomenon of adhesion is complex because of the many factors involved, such as surface free energy, viscoelasticity, and cohesion. Many studies have been conducted to investigate the nature of adhesion, most of which have focused on the various adhesion properties between spheres and substrates. In this study, we have investigated the adhesion characteristics between microscale spheres and rubber films with large thicknesses relative to the sphere diameters. Viscoelastic materials such as rubber generally require a long time to become wetted. To address this problem, we used spheres with sizes on the order of microns. For such small spheres, wetting at the surface proceeds in a sufficiently short time that we can observe the process. Therefore, we were able to observe deformation of the viscoelastic material caused by wetting. We focused on four main factors in order to investigate the process of adhesion, including two physical properties of the spheres, the surface free energy and the sphere size, in addition to the surface free energy, and viscoelasticity of rubber.

2. Experimental

Materials

cis-1,4-Polybutadiene rubber (BR) were used as an adhesive material. Silica, polystyrene (PS), and poly(methyl methacrylate) (PMMA) spheres were used for adhesion test. Diameters of these spheres were 5, 10, and 50 μm for silica, 12 μm for PS, and 8 μm for PMMA spheres.

Sample preparation and adhesion test of spheres with rubber surface

Thin rubber films with thickness around 500 nm was prepared by a spin cast method. Rubber films with large thickness compared to the diameter of the spheres were prepared by a solvent cast method. For thicker films, a crosslinked BR film was also made. The spheres were deposited onto the rubber films, then nitrogen gas was blown across the rubber surfaces to remove any unattached spheres. The interfacial area between the spheres and the rubber was imaged using scanning electron microscopy (SEM) after resting the samples for a designated length of time.

3. Results and discussion

Figure 1 shows an SEM image of the interface between a silica sphere with a 10 μm diameter and a BR film with a 500 nm thickness. The image clearly illustrates the formation of a BR meniscus on the silica sphere. Adhesion of the silica occurred quickly, in less than few seconds, so the rubber meniscus must have formed immediately after the spheres were deposited. Generally, contact between hydrophilic and hydrophobic materials tends to result in smaller contact areas; yet, the hydrophobic BR formed a meniscus on the hydrophilic silica surface.

Because the rubber meniscus formed on the spheres, we used thicker rubber films in place of the thin film to investigate the wetting process. These conditions resulted in sedimentation of the silica spheres into the rubber film. Figure 2 shows SEM images of this sedimentation, as well as similar sedimentation features for PS and PMMA spheres. The sedimentation ratio, δ/D, was calculated from SEM images to compare the sedimentation behavior of each sphere type, where the term δ is the sedimentation depth and D is the diameter of the spheres. Figure 3 shows the time-dependence of sedimentation for all three types of spheres. According to Figure 3, the sedimentation behavior indicated by the shape of the curves was nearly identical for all spheres. Additionally, the sedimentation velocities were also similar for all spheres, even for spheres with very different surface free energies. The sedimentation was caused by a meniscus force, F_{meniscus}, which acted on the sphere in the direction of the rubber film:

$$F_{\text{meniscus}} = F_{\text{Lap}} + F_{\text{cap}} = \pi r^2 \gamma_{\text{L}} \left(\frac{1}{R_1} + \frac{1}{R_2} \right) + 2\pi r \gamma_{\text{L}} \sin(\phi + \theta) \quad (R_1>0, R_2<0), \quad (1)$$

where F_{Lap} is a Laplace force caused by a Laplace pressure between rubber/air interface, F_{cap} is a capillary force working around the meniscus, γ_{L} is the surface tension of rubber film, r is the contact radius, and other parameters are shown in Figure 4a. The F_{meniscus} depends on the shape of meniscus and γ_{L}, and does not directly depend on the physical properties of the sphere, then the sedimentation behavior does not exhibit a strong dependence on the physical properties of the spheres.

Figure 3 also shows that sedimentation eventually ceased at a certain depth, depending on the type of sphere. The final depths were 85% for silica spheres, 95% for PS spheres, and 96% for PMMA spheres. The angle between the rubber surface and the tangential line to the sphere at its final position, θ_{end}, was calculated using δ/D at the final depth. These values were 45°, 26°, and 23°, respectively. To consider the factors that determine the final sedimentation position of the spheres, we assumed that θ_{end} was equal to the equilibrium contact angle, θ_{eq}, in Young's equation:

$$\gamma_{\text{S}} = \gamma_{\text{L}} \cos\theta_{\text{eq}} + \gamma_{\text{SL}}. \quad (2)$$

Here, γ_{S} and γ_{L} are the surface free energy of the solid and liquid, respectively, and γ_{SL} is the interfacial free energy between the liquid and the solid. For a sphere at the liquid–gas interface, the sphere is stable at the position where the forces on the tangential line around the contact line are balanced. Namely, in equilibrium, Young's equation is valid for the tangential line to the sphere. To verify whether this theory also held in our system, in which spheres were present at a viscoelastic material–gas interface, we determined θ_{eq} by the following experiment and compared the values of θ_{eq} with θ_{end}. Pieces of BR with an equilibrium contact area diameter of around 30 μm were placed on silica glass substrates. The final

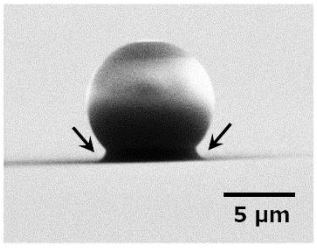

Figure 1. SEM image of the interface between a thin BR film and a silica sphere. 10 μm sphere diameter; 500 nm BR film thickness.

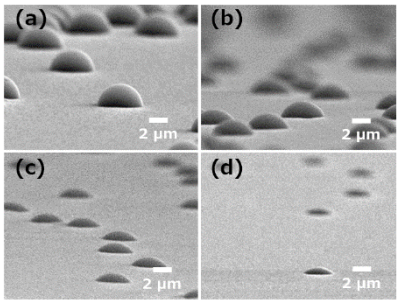

Figure 2. SEM images of PS spheres deposited on a thick BR film. 160 μm BR film thickness; 10 μm silica sphere diameter; resting times: (a) 5 min, (b) 30 min, (c) 10 h, and (d) 792 h.

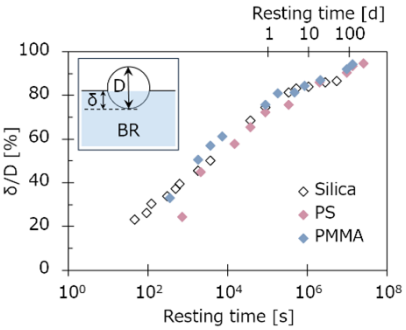

Figure 3. Resting-time-dependence of sedimentation ratios for silica, PS, and PMMA spheres in a thick BR film. Sphere diameters: silica 10 μm, PS 12 μm, and PMMA 8 μm; BR film thickness: 160 μm.

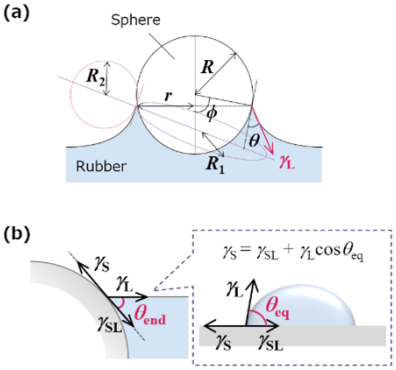

Figure 4. Schematics of (a) a meniscus between a sphere and rubber film and (b) a terminal contact angle θ_{end} and an equilibrium contact angle θ_{eq} in Young's equation.

contact angle reached a value of 43°, which was broadly consistent with the θ_{end} value of 45°. This result indicates that a sphere at a viscoelastic material–gas interface, as well as the liquid–gas system, is in equilibrium when θ_{end} becomes equal to θ_{eq} (Figure 4b).

We next confirm the influence of sphere size on the sedimentation behavior, various sizes of silica spheres were deposited onto a thick BR film. Figure 5a shows the time-dependence of sedimentation. The velocities clearly varied among the three spheres sizes, however, the final sedimentation ratios had very similar values. The plots in Figure 5a, with a reference sphere size of D = 50 μm, can be superposed on one another by shifting the data along the time axis (Figure 5b). In contrast to the velocity, the sedimentation behavior did not depend on sphere size (i.e., the curve shapes were nearly identical), as the shape of all plots were consistent. The final depth depended only on the physical properties of the spheres and the rubber: γ_S, γ_L, and γ_{SL}. The sphere size affected the velocity but not the overall behavior.

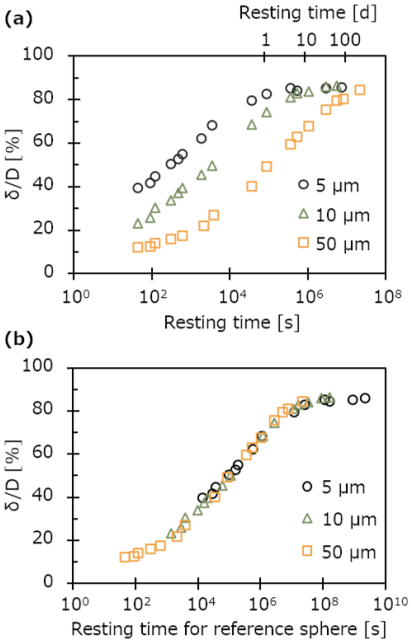

Figure 5. Resting-time-dependence of sedimentation ratios of silica spheres with various diameters in a thick BR film. (a) Raw data, (b) data shifted along the time axis. The reference sphere size is 50 μm.

As discussed above, the type of sphere did not affect the intermediate stage of sedimentation behavior, however the final sphere depth depended significantly on the material. Therefore, we considered the effect of different types of rubber. For this investigation, we observed the sedimentation behavior of silica spheres into crosslinked BR films. Figure 6 shows the time-dependence of sedimentation for silica spheres into crosslinked BR films. In contrast to above study, sedimentation behavior clearly varied according to rubber films. First, the surface free energy of BR0 (crosslinking time was 0 min) was nearly the same as that of BR15; however, the shear modulus increased with crosslinking time. Therefore, the flow of BR15 from the bottom to the side of a sphere and the sedimentation of BR15 were slower than that of BR0. This result suggests that the sedimentation velocity relies on the viscoelasticity of the rubber film. Secondly, BR30 clearly exhibited a different terminal sedimentation position than the other two samples. Because the surface free energy of BR30 was larger than those of BR0 and BR15, the positions predicted by Young's equation and thus the final depths were different. These results indicate that the sedimentation mechanism is strongly influenced by the physical properties of the rubber film, such as surface free energy and viscoelasticity.

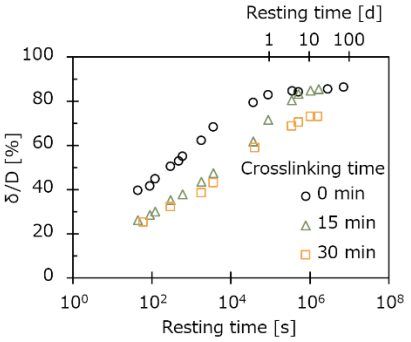

Figure 6. Resting-time-dependence of sedimentation ratios of silica spheres in a crosslinked BR film. 5 μm silica sphere diameter; 160 μm BR film thickness.

4. Conclusions

In this paper, we have reported the adhesion characteristics between microspheres and BR surfaces. In the case of the rubber films, with large thicknesses compared to the sphere diameters, sedimentation of the microspheres occurred. The driving force of sedimentation was the meniscus force. The sedimentation behavior mainly depended on the physical properties of the rubber, but it was nearly independent of the physical properties of the sphere. The sedimentation eventually stopped when Young's equation was valid on tangential line of sphere. In other words, the angle between the rubber surface and the tangential line of the sphere in its final position is equal to the equilibrium contact angle.